

DIFFERENTIAL GEOMETRY AND SPECTRAL ANALYSIS IN COMPUTER GRAPHICS

Alexander Pinzón Fernández

Advisor: Eduardo Romero

Bogotá-Colombia. October 2015



OUTLINE

Introduction

Proposed Method

Evaluation and Results

Products

Conclusions

INTRODUCTION

SPECTRAL MESH PROCESSING

Taubin in 1995 suggested that the **Discrete Laplace Operator** allows *Spectral Processing on Polygonal Meshes* in an analogous way to signal processing with the Fourier transform.

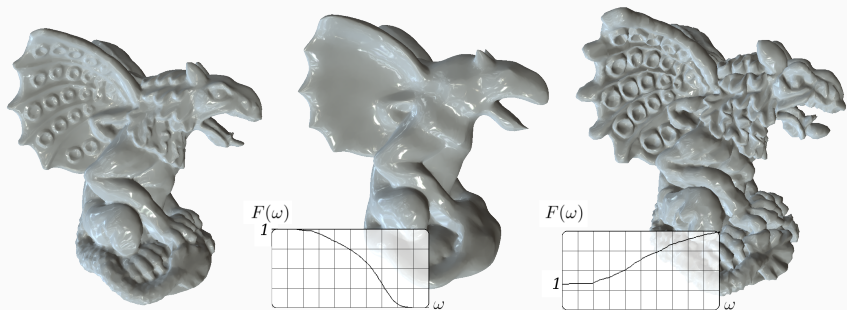


Figure: Original Mesh, Low-pass and enhancement filters [Vallet08].

LAPLACIAN OF THE FOURIER TRANSFORM

if u is a eigenfunction and λ is a corresponding eigenvalue of a linear differential operator A then

$$Au = \lambda u, \quad u \neq 0$$

LAPLACIAN OF THE FOURIER TRANSFORM

if \mathbf{u} is a eigenfunction and λ is a corresponding eigenvalue of a linear differential operator \mathbf{A} then

$$\mathbf{A}\mathbf{u} = \lambda\mathbf{u}, \quad \mathbf{u} \neq 0$$

The basis $\mathbf{e}_w = e^{2\pi iwx} = \cos(2\pi wx) - i \sin(2\pi wx)$ sine and cosine functions of the Fourier transform are eigenfunctions of the Laplacian with eigenvalue λ_w

$$\Delta(\mathbf{e}_w) = \frac{\partial^2}{\partial x^2} \mathbf{e}_w = -(2\pi w)^2 \mathbf{e}_w = \lambda_w \mathbf{e}_w$$

$$\Delta(\mathbf{e}_w) = \lambda_w \mathbf{e}_w$$

LAPLACE-BELTRAMI OPERATOR

The Laplace-Beltrami operator Δ_M is a differential operator given by the divergence of a gradient field on a **surface**.

$$\begin{aligned}\frac{\partial^2 f}{\partial x^2} + \frac{\partial^2 f}{\partial y^2} + \frac{\partial^2 f}{\partial z^2} &= 0 \\ \nabla_M^2 f &= \Delta_M = 0 \\ \Delta_M &= \text{div}(\nabla_M f)\end{aligned}$$

where M is a compact and smooth **Surface** (2D-Manifold).

LAPLACE-BELTRAMI OPERATOR

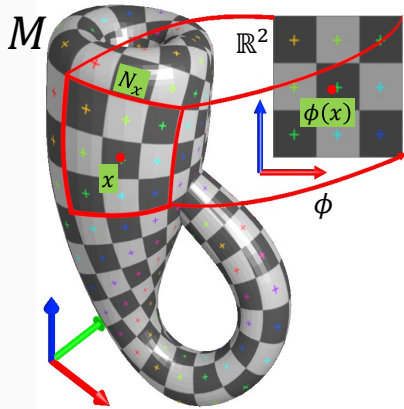
The Laplace-Beltrami operator Δ_M is a differential operator given by the divergence of a gradient field on a **surface**.

$$\begin{aligned}\frac{\partial^2 f}{\partial x^2} + \frac{\partial^2 f}{\partial y^2} + \frac{\partial^2 f}{\partial z^2} &= 0 \\ \nabla_M^2 f &= \Delta_M = 0 \\ \Delta_M &= \operatorname{div}(\nabla_M f)\end{aligned}$$

where M is a compact and smooth **Surface** (2D-Manifold).

The Laplace-Beltrami is a generalization of the Laplace operator for functions over surfaces and allows spectral surface analysis.

SURFACE



A Surface M is a 2D topological manifold.

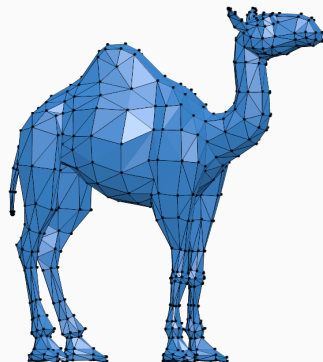
For which every point $x \in M \subseteq \mathbb{R}^3$ has a neighborhood N_x homeomorphic to euclidean space \mathbb{R}^2 .

A homeomorphism $\phi : N_x \rightarrow \mathbb{R}^2$

SURFACE DISCRETIZATION WITH POLYGONAL MESHES

In computer graphics a **Surface** is often discretized into a **Polygonal Mesh**

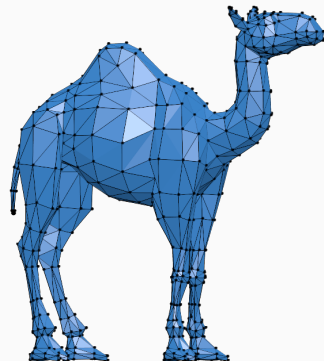
Polygonal Mesh is a set of points that are connected by **triangles** and **quads**.



SURFACE DISCRETIZATION WITH POLYGONAL MESHES

In computer graphics a **Surface** is often discretized into a **Polygonal Mesh**

Polygonal Mesh is a set of points that are connected by **triangles** and **quads**.



We need discrete versions of Laplacian operator to work with polygonal meshes.

DISCRETE LAPLACIAN OPERATOR AS A MATRIX EQUATION

The discrete version of Laplace operator for polygonal meshes.

Given a polygonal mesh $\mathbf{M} = [v_1, \dots, v_n]^T$ and $v_i \in \mathbb{R}^3$ we define the Discrete Laplacian operator matrix L with size $n \times n$

$$L(i,j) = \begin{cases} w_{ij} & \text{if } j \in N(v_i) \\ \sum w_{ik} & \text{if } i = j \\ 0 & \text{otherwise} \end{cases}$$

w_{ij} are the weights between the vertex v_i and vertex v_j . The weights are defined depending on the polygonal structure and application.

$N(v_i)$ is the 1-ring neighborhood with shared face to vertex v_i .

DESIRED PROPERTIES FOR LAPLACIAN MATRIX

This properties ensure the construction of eigenstructure of Laplacian matrix and then those eigenvectors of L matrix are an orthogonal basis of \mathbb{R}^n

- Symmetry.
- Square.
- Locality.
- Positive Weights.
- Positive Semi-Definiteness.
- Convergence.

EIGENSTRUCTURE OF LAPLACIAN MATRIX

$$L\mathbf{e}_i = \lambda_i \mathbf{e}_i, \quad \mathbf{e}_i \neq 0$$

- The eigenvector \mathbf{e}_i of L is a *natural vibration* of the mesh [Taubin95].
- The frequency of the wave \mathbf{e}_i is the eigenvalue λ_i of L that is the *natural frequency* [Taubin95].

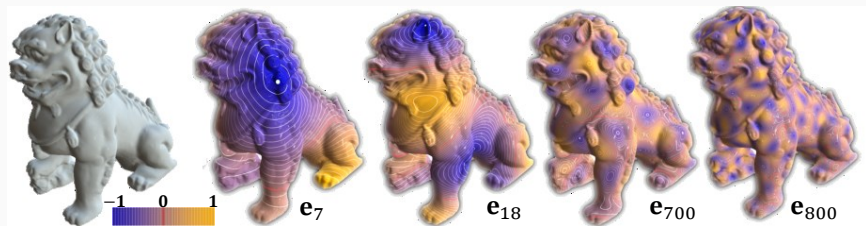


Figure: Color values are the amplitude of a wave \mathbf{e}_i projected on the mesh [Vallet08].

MESH RECONSTRUCTION

The mesh \mathbf{M} can be reconstructed from its spectral decomposition as the Fourier transform does.

$$\mathbf{M} = \sum_{i=1}^n \langle \mathbf{e}_i, \mathbf{M} \rangle \mathbf{e}_i$$

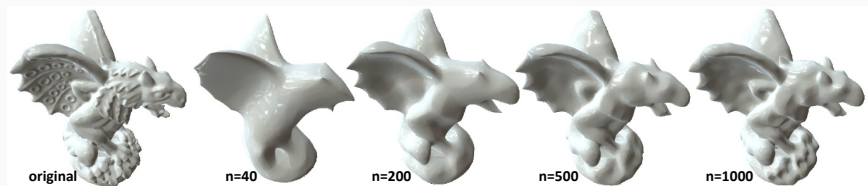


Figure: Mesh reconstruction with first n eigenvectors of the Discrete Laplacian Operator [Levy10].

WEIGHTS FOR LAPLACIAN OPERATOR

Desired property:

Non-negative weights ω_{ij} for $i \neq j$ ensure a positive semi-definite matrix.

- Umbrella Operator $w_{ij} = \begin{cases} 1 & \text{if } j \in N(v_i) \\ 0 & \text{else} \end{cases}$
- Fujiwara's Operator $w_{ij} = \begin{cases} \frac{1}{\|v_j - v_i\|} & \text{if } j \in N(v_i) \\ 0 & \text{else} \end{cases}$

1999 DESBRUN'S OPERATOR FOR TRIANGLE MESHES

This operator only works with meshes composed only by **triangles**.

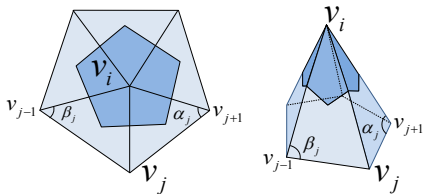
Desbrun's operator for
triangle meshes

$$\Delta(v_i) = 2\kappa_H \mathbf{n} = \frac{\nabla A}{A} = \frac{1}{A} * \frac{1}{2} \sum_j (\cot \alpha_j + \cot \beta_j)(v_i - v_j)$$

Mean curvature
normal

Area around v_i

Gradient of voronoi area ∇A



2011 XIONG'S MLBO OPERATOR FOR QUAD MESHES

This operator only work with meshes composed only by **quads**.

Xiong's operator for quad meshes

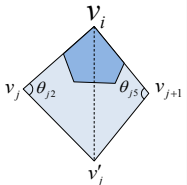
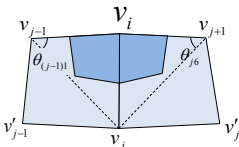
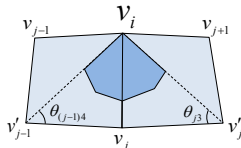
Primal triangulation

Dual triangulation

$$\Delta(v_i) = \frac{1}{A} * \frac{1}{2} \left[\sum_j w_{ij}(v_i - v_j) + \sum_{j'} w'_{ij}(v_i - v'_{j'}) \right]$$

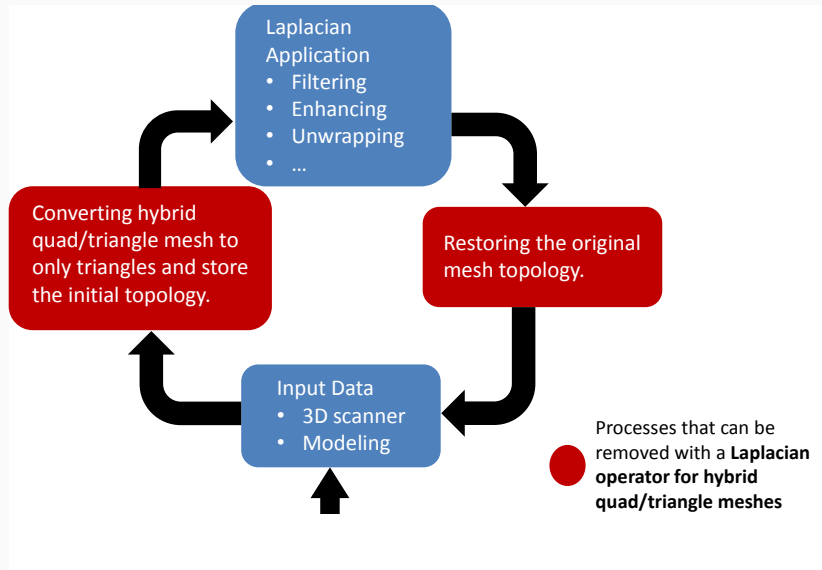
$$w_{ij} = \frac{1}{2} (\cot \theta_{(j-1)4} + \cot \theta_3) + \frac{1}{2} (\cot \theta_{(j-1)1} + \cot \theta_6)$$

$$w'_{ij} = \cot \theta_{j2} + \cot \theta_{j5}$$



LAPLACIAN APPLICATIONS ON 3D MODELING PROCESS

General 3D modeling process on polygonal meshes.



EDGE LOOPS FOR FACES

Hybrid quad/triangle meshes are necessary to 3D modeling artists

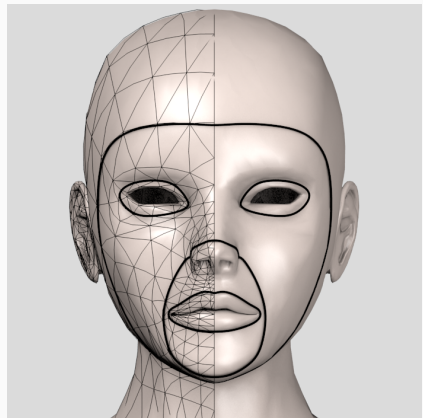


Figure: Triangle Mesh

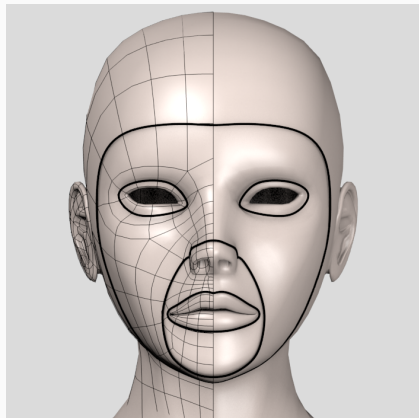
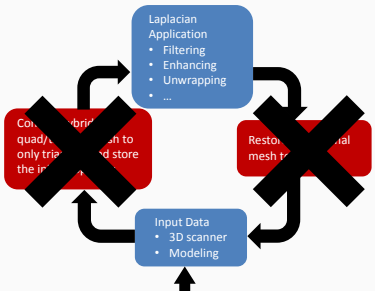


Figure: Hybrid Quad/Triangle Mesh

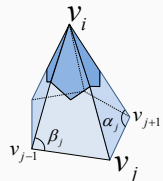
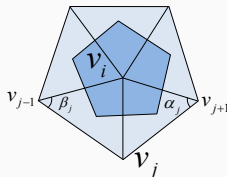
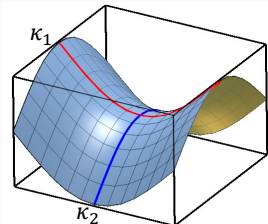
PROPOSED METHOD

OUR PROPOSAL

We propose an extension of the discrete Laplace-Beltrami operator to work with hybrid quad/triangle meshes and eliminate the need of triangulating the mesh and also allow the preservation of the original topology.



MATHEMATICAL FRAMEWORK OF OUR PROPOSAL



Curvature

$$\kappa = \frac{1}{R}$$

Mean Curvature

$$\kappa_H = \frac{\kappa_1 + \kappa_2}{2}$$

Discrete mean curvature normal

$$2\kappa_H \mathbf{n} = \frac{\nabla A}{A}$$

Laplace Beltrami operator

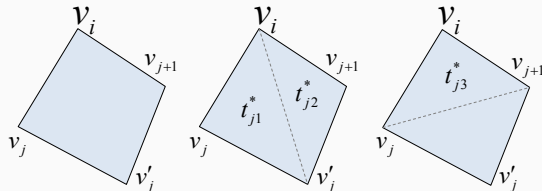
$$\Delta S = 2\kappa_H \mathbf{n}$$

Gradient of voronoi region

$$\nabla A = \frac{1}{2} \sum_j (\cot \alpha_j + \cot \beta_j)(v_i - v_j)$$

MATHEMATICAL FRAMEWORK OF OUR PROPOSAL

Xiong's mean average area



Mean Average
Area of all
triangulations of
quad Q around v_i

Primal
Triangulation
around v_i

Dual
Triangulation
around v_i

$$MAA(Q) = \frac{A_1 + A_2}{2} = \frac{A(t_{j1}^*) + A(t_{j2}^*) + A(t_{j3}^*)}{2}$$

LAPLACE BELTRAMI OPERATOR FOR HYBRID QUAD/TRIANGLE MESHES

Our proposal

Area of hybrid region with quads q_j and triangles t_k around v_i

$$A(v_i) = \sum_{j=1}^m A(q_j) + \sum_{k=1}^r A(t_k)$$

LAPLACE BELTRAMI OPERATOR FOR HYBRID QUAD/TRIANGLE MESHES

Our proposal

Area of hybrid region with quads q_j and triangles t_k around v_i

$$A(v_i) = \sum_{j=1}^m A(q_j) + \sum_{k=1}^r A(t_k)$$

Applying Xiong's mean average area for quads

$$A(v_i) = \frac{1}{2} \sum_{j=1}^m \left[A(t_{j1}^*) + A(t_{j2}^*) + A(t_{j3}^*) \right] + \sum_{k=1}^r A(t_k)$$

LAPLACE BELTRAMI OPERATOR FOR HYBRID QUAD/TRIANGLE MESHES

Our proposal

Area of hybrid region with quads q_j and triangles t_k around v_i

$$A(v_i) = \sum_{j=1}^m A(q_j) + \sum_{k=1}^r A(t_k)$$

Applying Xiong's mean average area for quads

$$A(v_i) = \frac{1}{2} \sum_{j=1}^m \left[A(t_{j1}^*) + A(t_{j2}^*) + A(t_{j3}^*) \right] + \sum_{k=1}^r A(t_k)$$

Applying Laplace operator

$$\Delta(v_i) = \frac{1}{2} \sum_{j=1}^m \left[\Delta(t_{j1}^*) + \Delta(t_{j2}^*) + \Delta(t_{j3}^*) \right] + \sum_{k=1}^r \Delta(t_k)$$

LAPLACE BELTRAMI OPERATOR FOR HYBRID QUAD/TRIANGLE MESHES

Our proposal

Area of hybrid region with quads q_j and triangles t_k around v_i

$$A(v_i) = \sum_{j=1}^m A(q_j) + \sum_{k=1}^r A(t_k)$$

Applying Xiong's mean average area for quads

$$A(v_i) = \frac{1}{2} \sum_{j=1}^m \left[A(t_{j1}^*) + A(t_{j2}^*) + A(t_{j3}^*) \right] + \sum_{k=1}^r A(t_k)$$

Applying Laplace operator

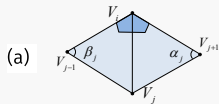
$$\Delta(v_i) = \frac{1}{2} \sum_{j=1}^m \left[\Delta(t_{j1}^*) + \Delta(t_{j2}^*) + \Delta(t_{j3}^*) \right] + \sum_{k=1}^r \Delta(t_k)$$

Rewriting $\Delta(v_i)$ we define the *Triangle Quad Laplace Beltrami Operator*

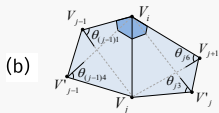
$$\Delta(v_i) = \frac{1}{2A_i} \sum_{j=1}^m w_{ij} (v_j - v_i)$$

WEIGHTS FOR TQLBO - OUR PROPOSAL

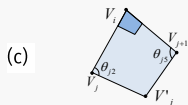
The 5 basic triangle-quad cases with a vertex V_i and the relationship with V_j and V'_j



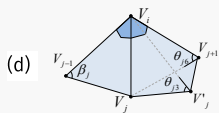
$$w_{ij} = \cot \theta_{j2} + \cot \theta_{j5}$$



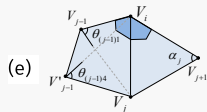
$$w_{ij} = \frac{1}{2}(\cot \theta_{(j-1)4} + \cot \theta_3) + \frac{1}{2}(\cot \theta_{(j-1)1} + \cot \theta_6)$$



$$w_{ij} = \cot(\alpha_j) + \cot(\beta_j)$$



$$w_{ij} = \frac{1}{2}(\cot \theta_{j3} + \cot \theta_{j6}) + \cot \beta_j$$



$$w_{ij} = \frac{1}{2}(\cot \theta_{(j-1)1} + \cot \theta_{(j-1)4}) + \cot \alpha_j$$

LAPLACE OPERATOR AS A MATRIX EQUATION

Our proposal

We define a TQLBO as a matrix equation

$$L(i,j) = \begin{cases} -\frac{1}{2A_i} w_{ij} & \text{if } j \in N(v_i) \\ \frac{1}{2A_i} \sum_{k \in N(v_i)} w_{ik} & \text{if } i = j \\ 0 & \text{otherwise} \end{cases} \quad (1)$$

Where L is an $n \times n$ matrix, n is the number of vertices , $N(v_i)$ is the 1-ring neighborhood with shared face to v_i , A_i is the ring area around v_i .

EVALUATION AND RESULTS

A standard diffusion process is used.

$$\frac{\partial V}{\partial t} = \lambda L(V)$$

To solve this equation, implicit integration is used as well as a normalized version of TQLBO matrix

$$(I - |\lambda dt| W_p L) V' = V^t$$

$$V^{t+1} = V^t + \text{sign}(\lambda) (V' - V^t)$$

where L is the TQLBO, V' are the smoothing vertices, V^t are the actual vertices positions, W_p is a diagonal matrix with vertex weights, and λdt is the inflate factor.

SCULPTING WITH ENHANCING FILTER

Inflate Brush

Real-time brushes require the Laplacian matrix be constructed with the vertices that are within the sphere radius defined by the user, reducing the matrix to be processed.

$$L(i,j) = \begin{cases} -\frac{w_{ij}}{\sum\limits_{j \in N(v_i)} w_{ij}} & \text{if } \|v_i - u\| < r \wedge \|v_j - u\| < r \\ 0 & \text{if } \|v_i - u\| < r \wedge \|v_j - u\| \geq r \\ \delta_{ij} & \text{otherwise} \end{cases}$$

Where $v_j \in N(v_i)$, u is the sphere center of radius r . The matrices should remove rows and columns of vertices that are not within the radius.

COMPUTE THE MINIMAL SURFACE WITH TQLBO RESULTS

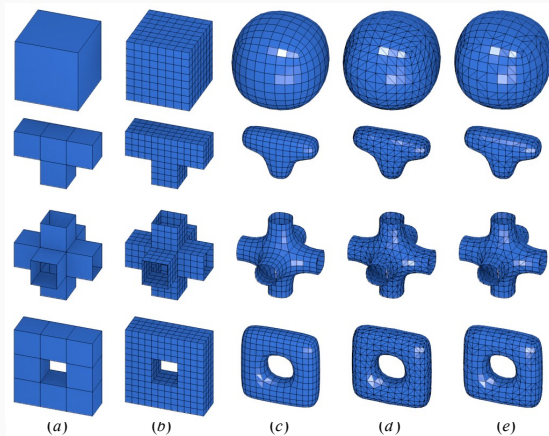


Figure: (a) Original Model. (b) Simple subdivision. (c), (d) (e) Laplacian smoothing with $\lambda = 7$ and 2 iterations: (c) for quads, (d) for triangles, (e) for triangles and quads randomly chosen.

SHAPE INFLATION WITH ENHANCING FILTER RESULTS

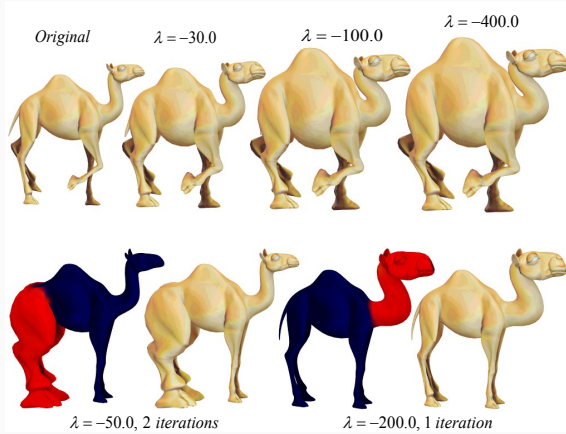


Figure: Top row: Original camel model on left. Shape inflation with $\lambda = -30.0$, $\lambda = -100.0$, $\lambda = -400.0$. Bottom row: Shape inflation with weight vertex group, $\lambda = -50.0$ and 2 iterations for the legs, $\lambda = -200.0$ and 1 iteration for head and neck.

INFLATE BRUSH RESULTS

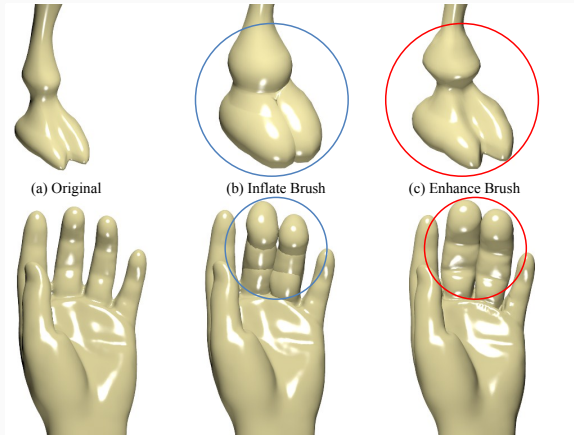


Figure: Top row: (a) Leg Camel, (b) Traditional inflate brush for leg into blue circle, (c) Shape inflation brush for leg into red circle. Bottom row: (a) Hand, (b) Traditional inflate brush for fingers into blue circle, (c) Shape inflation brush for fingers in red circle.

INFLATE BRUSH PERFORMANCE

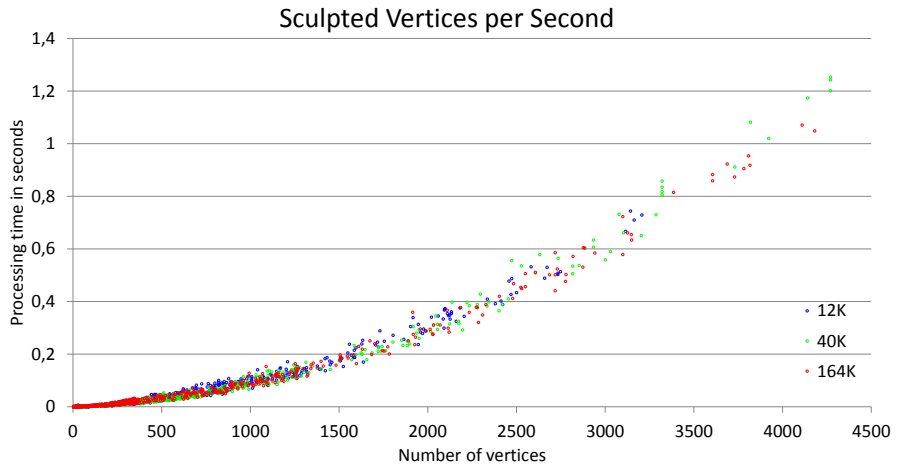


Figure: Performance of our dynamic shape inflation brush in terms of the sculpted vertices per second. Three models with 12K, 40K, 164K vertices used for sculpting in real time.

PRODUCTS

Shape Inflation With an Adapted Laplacian Operator For Hybrid Quad/Triangle Meshes

Alexander Pinzon, Eduardo Romero

Cimalab Research Group

Universidad Nacional de Colombia

Bogota-Colombia

Email: apinzonf@unal.edu.co, edromero@unal.edu.co



Fig. 1. A set of 48 successive shapes enhanced, from $\lambda = 0.0$ in blue to $\lambda = -240.0$ in red, with steps of -5.0 .

Abstract—This paper proposes a novel modeling method for a hybrid quad/triangle mesh that allows to set a family of possible shapes by controlling a single parameter, the global curvature. The method uses an original extension of the Laplace Beltrami operator that efficiently estimates a curvature parameter which is used to define an inflated shape after a particular operation performed in certain mesh points. Along with the method, this work presents new applications in sculpting and modeling, with subdivision of surfaces and weight vertex groups. A series of graphics examples demonstrates the quality, predictability and flexibility of the method in a real production environment with software Blender.

Keywords-laplacian smooth; curvature; sculpting; subdivision surface

[12]. Nevertheless these methods are difficult to deal with since they require a large number of parameters and a very tedious customization. Instead, the presented method requires a single parameter that controls the global curvature, which is used to maintain realistic shapes, creating a family of different versions of the same object and therefore preserving the detail of the original model and a realistic appearance.

Interest in meshes composed of triangles and quads has lately increased because of the flexibility of modeling tools such as Blender 3D [13]. Nowadays, many artists use a manual connection of a couple of vertices to perform animation processes and interpolation [14]. It is then of paramount

2ND PRODUCT - AWARDED INTERNSHIP

Mesh smoothing based on curvature flow operator in a diffusion equation

Sponsor: Google Inc - Google Summer of Code 2012 program

Project: Mesh smoothing based on curvature flow operator in a diffusion equation

Synopsis: This project proposes a new and robust mesh smoothing tool that removes the noise on the surfaces of models captured with 3d scanners, zcameras among others.

Blender: This software is an open source 3D application for modeling, rendering, composing, video editing and game creation.

2ND PROD - LAPLACIAN SMOOTH TOOL FOR BLENDER

Mesh smoothing based on curvature flow operator in a diffusion equation

We define a Laplacian matrix for mesh smoothing with support for hybrid quad/triangle meshes with holes as

$$L(i, j) = \begin{cases} -\frac{1}{2A_i} W_{ij} & \text{if } j \in N(v_i) \wedge v_i \notin \text{Boundary} \\ \frac{1}{2A_i} \sum_{j \in N(v_i)} W_{ij} & \text{if } i = j \wedge v_i \notin \text{Boundary} \\ -\frac{1}{\|v_i - v_j\|} & \text{if } j \in N(v_i) \wedge \{v_i, v_j\} \in \text{Boundary} \\ \frac{2}{E_i} \sum_{j \in N(v_i)} \frac{1}{\|v_i - v_j\|} & \text{if } i = j \wedge \{v_i, v_j\} \in \text{Boundary} \\ 0 & \text{otherwise} \end{cases}$$

w_{ij} is the TQLBO defined in equation (1)

$$E_i = \sum_{j \in N(v_i)} e_{ij} .$$

2ND PRODUCT - USER INTERFACE

Mesh smoothing based on curvature flow operator in a diffusion equation

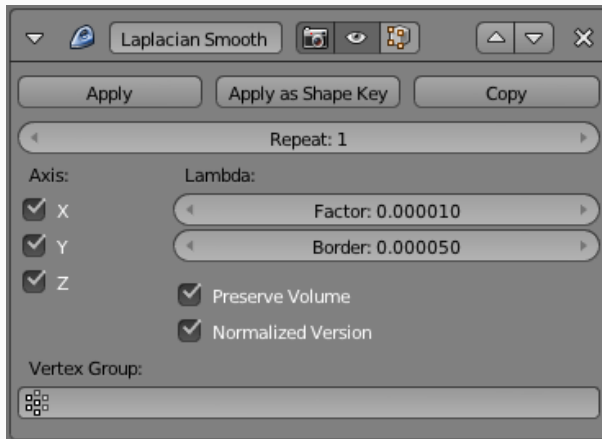


Figure: Panel inside blender user interface of the Laplacian Smooth modifier tool.

2ND PRODUCT - RESULTS

Mesh smoothing based on curvature flow operator in a diffusion equation

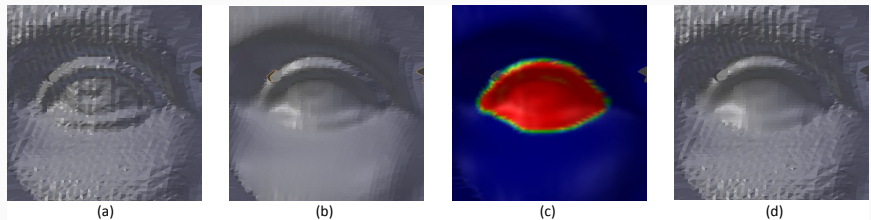


Figure: Use of weights per vertex to constrain the effect of mesh smoothing. (a) Original Model. (b) Smoothing with $\lambda = 1.5$. (c) Red vertices $weight = 1.0$, blue vertices $weight = 0.0$. (d) Smoothing with $\lambda = 2.5$. Red vertices were the only vertices smoothed.

2ND PRODUCT - RESULTS

Mesh smoothing based on curvature flow operator in a diffusion equation

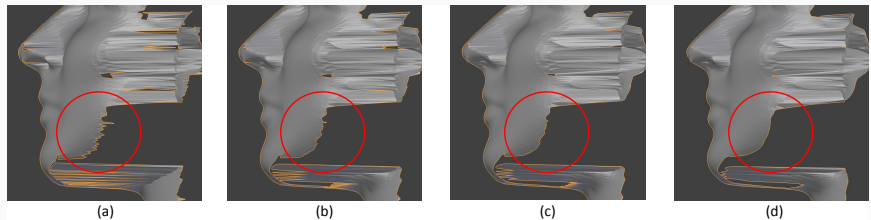


Figure: Smoothing boundary changing λ_{Border} factor. (a) Original Model. (b) Smoothing $\lambda_{Border} = 1.0$. (c) Smoothing $\lambda_{Border} = 2.5$ (d) Smoothing with $\lambda_{Border} = 10.0$.

3RD PRODUCT - AWARDED INTERNSHIP

Mesh Editing with Laplacian Deform

Sponsor: Google Inc - Google Summer of Code 2013 program

Project: Mesh Editing with Laplacian Deform

Synopsis: This project proposes a new tool that allows to pose a mesh while preserving geometric details of the surface.

Blender: This software is an open source 3D application for modeling, rendering, composing, video editing and game creation.

3RD PRODUCT - DIFFERENTIAL COORDINATES

Mesh Editing with Laplacian Deform

$$\delta_i = \sum_{j=1}^m w_{ij} (v_i - v_j) \quad (2)$$

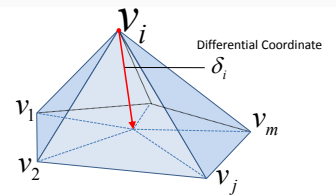


Figure: Difference between v_i and the center of mass of its neighbors v_1, \dots, v_m .

w_{ij} is the TQLBO defined in equation (1)

3RD PRODUCT - LAPLACIAN DEFORM

Mesh Editing with Laplacian Deform

The linear system for finding the new pose of a mesh is

$$\begin{bmatrix} L \\ W_c \end{bmatrix} V = \begin{bmatrix} \delta \\ W_c C \end{bmatrix} \quad (3)$$

L is a matrix that used our TQLBO defined in equation (1).

W_c is a matrix that has only ones in the indices of anchor vertices.

V is a vector with the vertices of the mesh positions.

C is a vector with coordinates of anchor vertices after several manual transformations.

δ is the differential coordinates defined in equation (2).

3RD PRODUCT - USER INTERFACE

Mesh Editing with Laplacian Deform

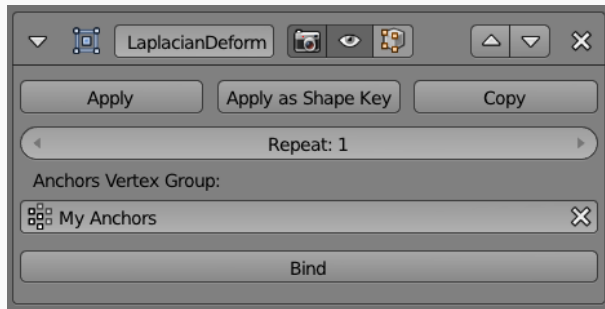


Figure: Panel inside Blender user interface of the Laplacian Deform modifier tool.

3RD PRODUCT - RESULTS

Mesh Editing with Laplacian Deform

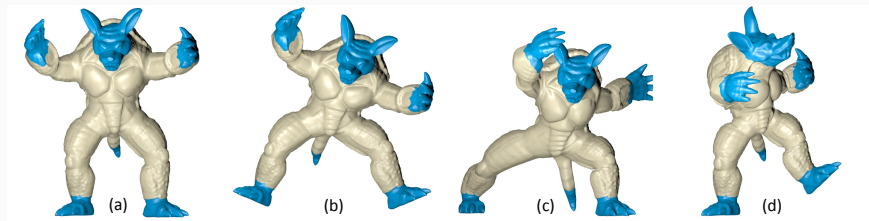


Figure: Anchor vertices in blue. (a) Original Model, (b,c,d) new poses only change the anchor-vertices. The system finds positions for vertices in yellow.

3RD PRODUCT - RESULTS

Mesh Editing with Laplacian Deform

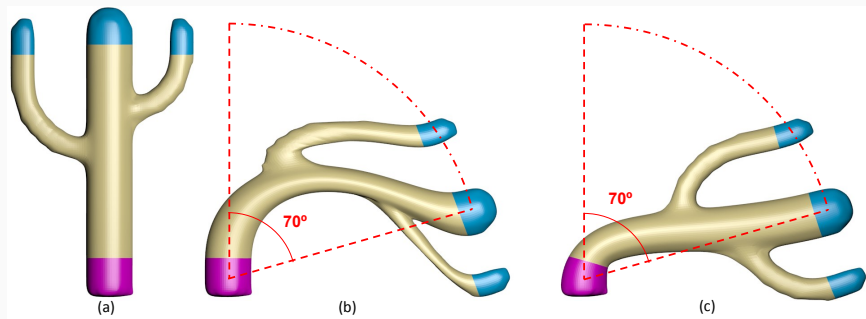


Figure: (a) Original cactus model. (b) Blue segments are rotated 70° to the right and, afterwards, a basic interpolation is applied to parts in yellow (c) Blue segments are rotated 70° to the right and, afterwards, a Laplacian deform tool is applied to parts in yellow.

3RD PRODUCT - RESULTS

Mesh Editing with Laplacian Deform

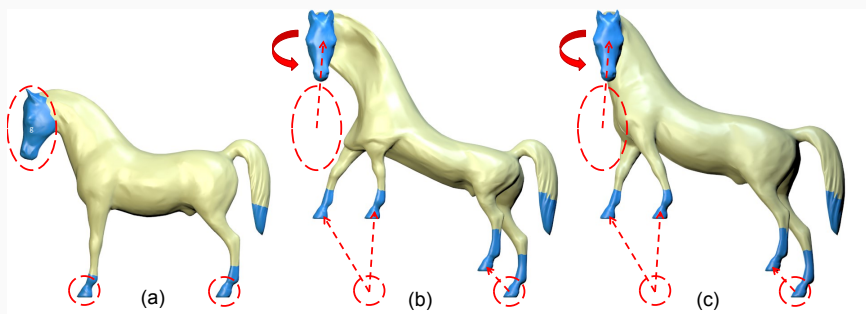


Figure: (a) Original Horse model. (b) Blue segments are translated and rotated and then basic interpolation is applied to the yellow parts (c) Blue segments are translated and rotated and then the Laplacian Deform tool is applied to the yellow parts.

4TH PRODUCT - POSTER

6th International Seminar on Medical Image Processing and Analysis SIPAIM 2010

Análisis Experimental de la Extracción del Esqueleto por Contracción con Suavizado Laplaciano

Alexander Pizán, Fabio Martínez, Eduardo Romano

Abstract

Este artículo presenta un análisis estadístico del método de extracción del esqueleto por medios de la contracción de un volumen con suavizado Laplaciano. El trabajo realiza una evaluación experimental al problema de la extracción del esqueleto, para medir el rendimiento del método Frenet a través de comparaciones, y discute la base de simplificación.

Diseño evaluativo utilizó el modelo tridimensional animado de una persona que realizaba una caminata, a modo modelo se le extrajo el esqueleto y se compararon las diferencias en dibujos instantáneos de la extracción, y distintas configuraciones del proceso de simplificación. Los resultados muestran un sólido rendimiento del método Frenet a los buenas diferencias entre la extracción y muestra preferencia en la base de simplificación de esqueleto.



Contracción con Suavizado Laplaciano

Este método consiste básicamente una red de polígonos por medio del suavizado laplaciano hasta tener un volumen de un figura 1. Los vértices de la red tienen una tasa constante de producción de energía, con los siguientes bloques:

$$W_1(D)^2 + \sum W_2_i B^i - V_i^2$$

- Operador Laplaciano para remover las irregularidades, es decir suavizar las formas de la geometría.
- Mín. Fuerza de atracción que usa los vértices, para mantener información clara de la geometría.
- Mín. Fuerza de contracción que hace la forma tridimensional puro volumen.



Referencias y Agradecimientos

- Daeil Kim-Chung, So, Cheon-Jae Lee, Taek-Hwan Kim, Chon-Gyu Cho, Daniel Cohen-Or, and Tong-Yee Li. Multi-view skeleton extraction via multi-view depth maps. *IEEE Transactions on Pattern Analysis and Machine Intelligence*, 32(11):2010–2020, December.
- Daeil Kim-Chung, So, Cheon-Jae Lee, and Insoo Hwang. Articulated multi-view skeleton extraction from multi-view silhouettes. *ACM Trans. Graph.*, 27(3):1–20, 2008. 10
- Ramanerri, C. and Patrick M. Cesar. *Surface processing, applications, and algorithms*. IEEE Transactions on Pattern Recognition and Computer Graphics, 17(2):630–642, 2003.
- Agradecimientos: The original performance data were provided courtesy of the Computer Graphics Group of the NTT CSRD, Japan Research (Cambridge, Japón).

Implementación

Se usó la implementación hecha en C# del Dr. Chung Su et al. Para los sujetos, para realizar la extracción del esqueleto de un modelo tridimensional que fue obtenido mediante la captura de imágenes de la cámara web que se realizó en la Universidad de Monterrey por Pérez et al. De este modelo se registró una caminada durante 200 cuadros. Se realizó la extracción del esqueleto en cada cuadro y se obtuvo una base de datos para describir un esqueleto (ver figura 2) y se clasificaron los sujetos así en figura 3.

En el segundo experimento se seleccionaron algunos punto para obtener la complejidad topológica entre los esqueletos medidos y analizar el complemento del método Frenet a transformaciones isométricas de la geometría de un cuerpo.

Resultados

El método logra el mejor ajuste al esqueleto de un cuerpo. Los transformaciones isométricas, en la tabla 2, se recuperaron en promedio 13.71% de los 22 necesarios para la rectificación de imágenes en diferentes tipos de esqueletos. La media de los errores es 2.86 milímetros y se observó regularmente la extracción del esqueleto. La línea verde en la figura 3 describe el número de nodos que hacen falta para conseguir el esqueleto.



Durante la fase de simplificación (ver figura 2) el método no sufre perdida ni en precisión de los nodos de 22 nodos (base real). El método tiene una alta eficiencia en la extracción de los 22 nodos y su rendimiento es similar al de la base real de la figura 3.

Conclusiones y Trabajo Future

El método de extracción resulta más eficiente y tiene bajo impacto frente a cambios sutiles de la geometría; el método puede trabajar de forma automática o a lo largo de los cuadros. El método recupera de forma eficiente los nodos de un esqueleto, alternando la extracción de nodos de la pieza. El método provee resultados de forma sencilla y esférica de segmentación del esqueleto a lo largo del tiempo.

Como trabajo futuro es posible mejorar la recuperación de información haciendo que la cohärenza espacial temporal no presente en la técnica de extracción, para lograr la recuperación de la información de los nodos de los esqueletos. Es posible probar el uso de algoritmos de partición de nodos.

5TH PRODUCT - POSTER

7th International Seminar on Medical Image Processing and Analysis SIPAIM 2011

Software para la Extracción del Esqueleto por Contracción y Suavizado

Alexander Pineda, Eduardo Romero

Abstract

Este artículo propone un software para el procesamiento, visualización e implementación del esqueleto de mallas tridimensionales. El sistema se compone con base en un sistema de plugins y filtros, se implementó un plugin que contiene un filtro para la extracción del esqueleto por contracción en dirección gradiente con suavizado Laplaciano. El software producido proporciona una plataforma flexible para el diseño e implementación de plugins.

Métodos de Suavizado de Mallas

Los métodos para suavizar mallas reducen el ruido, o permiten iterativamente eliminar frecuencias altas presentes en el muestreo tridimensional de los modelos.

Método Laplaciano

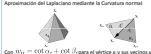
La idea básica consiste en mover un vértice en la $E_0(1) = \frac{\partial X}{\partial s}$ misma dirección del Laplaciano.

La ecuación 1 se implementa como la ecuación de diferencias hacia adelante es: $E_0(2) X_{i+1} = (I + \lambda L)X_i$. Donde X es el conjunto de vértices, L es el Laplaciano, y $\lambda \in \mathbb{R}$ es la velocidad de difusión.

Y la aproximación discreta de la ecuación 2 es:

$$E_0(3) L(x_i) = \sum_{j \in V_i} \{x_j - x_i\} \quad x_j \in \text{Vecinos}(x_i)$$

Aproximación del Laplaciano mediante la Curvatura normal



Software Skeletonizer



Contacto

Alexander Pineda Fernández alexander.pineda@unal.edu.co
Grupo de Investigación Biogenium <http://biogenium.unal.edu.co>
Universidad Nacional de Colombia www.unal.edu.co
Facultad de Medicina, Edificio 471 Primer Piso

Implementación para la extracción del esqueleto

La Esqueletización reduce la dimensionalidad y representa un cuerpo como un estructura unidimensional.

El esqueleto puede ser obtenido suavizando la malla pero bajo dos restricciones que da prioridad al Laplaciano y que mantiene los vértices en su localización original.

Extracción del esqueleto: $\begin{bmatrix} W_1, L \\ W_2, L \end{bmatrix} X_{i+1} = \begin{bmatrix} 0 \\ W_H K_i \end{bmatrix}$

Donde $W_1L = \text{Suavizado de Laplaciano con } w_1$, $w_1 = \cot \alpha_f + \cot \beta_f$ basado en la curvatura de fuga

Y la nueva restricción propuesta en este trabajo



Tratar de suavizar los vértices a lo largo de la linea

La distancia del punto a la linea: $d = \vec{P}_1 + t\vec{P}_2$, donde P_1, P_2 :=el extremo(líne, $P_0) = \frac{(P_0-P_1)(x(P_0)-P_1)}{|P_1-P_2|}$

Cada punto en un plano satisface esta ecuación

$$P_0 : \alpha x + \beta y + \gamma z + d_0 = 0.$$

Resultados



Los vértices se pueden mover a lo largo de la linea.

• El esqueleto tiene muchas ramas.

• Los vértices no tienen buenas posiciones.

• La solución debe ser restringida a una región particular de la linea.

Referencias y Agradecimientos

- Chia-Kin Chang Au, Chia-Lin Tsai, Hung-Kuo Chu, Daniel Cohen-Or, and Yung-Huei Lin. 2008. Multi-scale skeleton extraction. *ACM Trans. Graph. Comput. Graph. Interact. Techniques*, 27(3) 33, 2008. Skeleton Extraction.
- Daniel Vitru, Ayu Irawan, Majisch Mittalas, and Zdenek Popovic. Articulated mesh skeletons with multi-level constraints. *ACM Trans. Graph. Comput. Graph. Interact. Techniques*, 27(3) 33, 2008. Skeleton Extraction.
- De Corato, Giacomo M. Curve skeleton extraction, applications, and algorithms. *Ph.D. Thesis*, Univ. Milano, Italy, 2007.
- Agapiou, J. and Frerichs, M. A. Vertex skeletonization and compact representations, 1, 160–164, 2007. Skeleton Extraction Survey. Melenikov, Sverl, Delcambre.

Agradecimientos: The captured performance data were provided courtesy of the Computer Graphics Group of the MIT CSAIL Vision Research (Cambridge, USA).



5TH PRODUCT - SKELETON EXTRACTION

Software para la Extracción del Esqueleto por Contracción y Suavizado

Au et al. [Au2008] propose the next system of equations to iteratively contract the mesh until the volume is zero. Next, a simplification process is done and a skeleton appears.

$$\begin{bmatrix} W_L L \\ W_H \end{bmatrix} X_{t+1} = \begin{bmatrix} 0 \\ W_H X_t \end{bmatrix} \quad (4)$$

L is a matrix that used our TQLBO defined in equation (1).

W_L is a diagonal weighting matrix for the smoothing factor.

W_H is a diagonal weighting matrix for the attraction constraint factor.

A_i^t and A_i^0 are the current area and initial area of the ring surrounding x_i .

UNDESIRABLE DISPLACEMENT OF NODES FROM ROTATIONAL CENTER

5th product - Poster

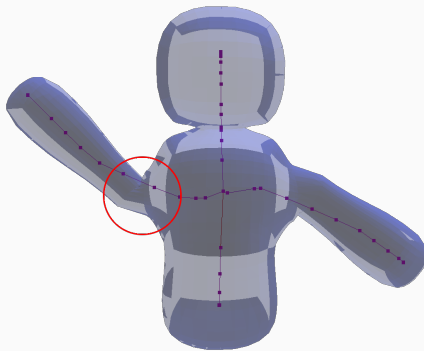


Figure: Skeleton that has a node outside its rotational center.

5TH PRODUCT - CONTRIBUTION

Software para la Extracción del Esqueleto por Contracción y Suavizado

The basic idea is to move the vertices along a normal line, estimated at every vertex, based on the average of the normal of the faces.

This constraint eliminates the need to adjust the final skeleton.

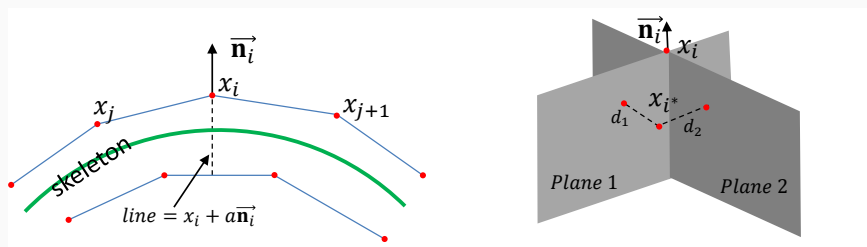


Figure: Left: The vertex x_i moves along the line constraint. Right: the distance of vertex x_i to plane 1 and plane 2 when the position in every iteration changes.

THE DISTANCE EQUATION OF POINT p TO PLANE Π

5th product - Poster

The plane equation

$$ax + b_0y + c_0z + d_0 = 0$$

The distance of point $P_0 = \{x_0, y_0, z_0\}$ to a plane $\Pi = ax + b_0y + c_0z + d_0$.

$$|\Pi - P_0| = \frac{|ax_0 + by_0 + cz_0 + d|}{\sqrt{a^2 + b^2 + c^2}} \quad (5)$$

5TH PRODUCT - THE NEW SYSTEM OF EQUATIONS PROPOSED

Software para la Extracción del Esqueleto por Contracción y Suavizado

$$\begin{bmatrix} W_L L \\ W_H \\ \Pi_1 \\ \Pi_2 \end{bmatrix} X_{t+1} = \begin{bmatrix} 0 \\ W_H X_t \\ -D_1 \\ -D_2 \end{bmatrix} \quad (6)$$

Π_1 and Π_2 are matrices that contain a, b, c values of the plane equation for every vertex.

D_1 and D_2 are the vectors with d values of the plane equation for every vertex.

5TH PRODUCT - USER INTERFACE

Software para la Extracción del Esqueleto por Contracción y Suavizado

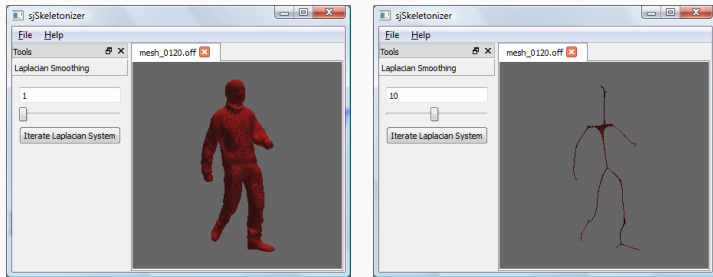


Figure: sjSkeletonizer is our prototype software application

As a result of this work, the software sjSkeletonizer permits the processing, visualization and extraction of the skeleton from polygonal hybrid meshes composed of triangles and quads.

5TH PRODUCT - RESULTS

Software para la Extracción del Esqueleto por Contracción y Suavizado

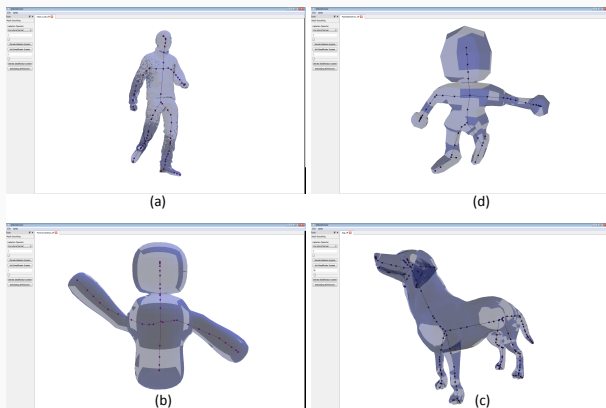


Figure: Skeletons extracted from different models. (a) Dog model (b) Character model. (c) Person model. (d) Clay model.

5TH PRODUCT - RESULTS

Software para la Extracción del Esqueleto por Contracción y Suavizado

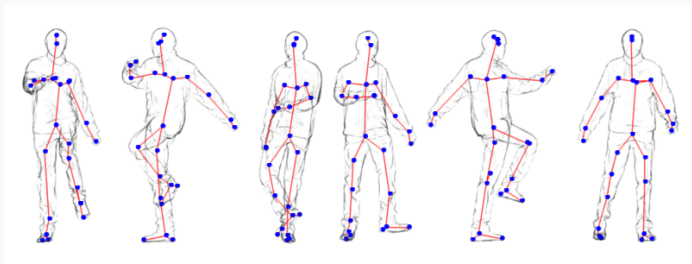


Figure: Model with different poses and skeleton obtained with our skeleton extraction software.

CONCLUSIONS

CONCLUSIONS

- This work presented a novel extension of the Laplace Beltrami operator for hybrid quad/triangle meshes, and the successful application of such principles in different types of problems in computer geometric modeling like smoothing, enhancing, sculpting, deformation, reposing and skeleton extraction.

CONCLUSIONS

- This work presented a novel extension of the Laplace Beltrami operator for hybrid quad/triangle meshes, and the successful application of such principles in different types of problems in computer geometric modeling like smoothing, enhancing, sculpting, deformation, reposing and skeleton extraction.
- A new sculpting brush to made a proper inflation while preserving the geometric details in real-time sessions was proposed, implemented and tested.

CONCLUSIONS

- This work presented a novel extension of the Laplace Beltrami operator for hybrid quad/triangle meshes, and the successful application of such principles in different types of problems in computer geometric modeling like smoothing, enhancing, sculpting, deformation, reposing and skeleton extraction.
- A new sculpting brush to make a proper inflation while preserving the geometric details in real-time sessions was proposed, implemented and tested.
- We have largely demonstrated that our method has a good performance, stability and robustness of the extension proposed.

CONCLUSIONS

- This work presented a novel extension of the Laplace Beltrami operator for hybrid quad/triangle meshes, and the successful application of such principles in different types of problems in computer geometric modeling like smoothing, enhancing, sculpting, deformation, reposing and skeleton extraction.
- A new sculpting brush to make a proper inflation while preserving the geometric details in real-time sessions was proposed, implemented and tested.
- We have largely demonstrated that our method has a good performance, stability and robustness of the extension proposed.
- This novel extension of the Laplace Beltrami operator was introduced in the computer modeling industry inside the Blender 3D computer graphics software.

ACKNOWLEDGMENT

- We would like to thank CIM@LAB Research Group for their support on our research.
- This work was supported in part by the Blender Foundation, Google Summer of code program in 2012 and 2013.
- Livingstone elephant model was provided by courtesy of INRIA and ISTI by the AIM@SHAPE Shape Repository. Hand model was courtesy of the FarField Technology Ltd. Camel model by Valera Ivanov is licensed under a Creative Commons Attribution 3.0 Unported License. Dinosaur and Monkey models are under public domain, courtesy of Blender Foundation.

BIBLIOGRAPHY I

-  Oscar Kin-Chung Au, Chiew-Lan Tai, Hung-Kuo Chu, Daniel Cohen-Or, and Tong-Yee Lee.
Skeleton extraction by mesh contraction.
ACM Transactions on Graphics, 27(3):10, 2008.
-  Blender-Foundation.
Blender open source 3d application for modeling, animation, rendering, compositing, video editing and game creation.
<http://www.blender.org/>, 2012.
-  Mario Botsch, Leif Kobbelt, Mark Pauly, Pierre Alliez, and Bruno Lévy.
Polygon mesh processing.
CRC press, 2010.
-  Mathieu Desbrun, Mark Meyer, Peter Schroder, and Alan H. Barr.
Implicit fairing of irregular meshes using diffusion and curvature flow.
In *SIGGRAPH '99: Proceedings of the 26th annual conference on Computergraphics and interactive techniques*, pages 317–324, New York, NY, USA, 1999. ACM Press/Addison-Wesley Publishing Co.
-  Michael S. Floater.
Mean value coordinates.
Computer Aided Geometric Design, 20(1):19 – 27, 2003.

BIBLIOGRAPHY II

-  Bruno Lévy and Hao (Richard) Zhang.
Spectral mesh processing.
In *ACM SIGGRAPH 2010 Courses*, SIGGRAPH '10, pages 8:1–8:312, New York, NY, USA, 2010. ACM.
-  Mark Meyer, Mathieu Desbrun, Peter Schroder, and Alan H. Barr.
Discrete differential-geometry operators for triangulated 2-manifolds.
In Hans-Christian Hege and Konrad Polthier, editors, *Visualization and Mathematics III*, pages 35–57. Springer-Verlag, Heidelberg, 2003.
-  Tony Mullen.
Introducing character animation with Blender.
Indianapolis, Ind. Wiley Pub. cop., 2007.
-  Ulrich Pinkall, Strasse Des Juni, and Konrad Polthier.
Computing discrete minimal surfaces and their conjugates.
Experimental Mathematics, 2:15–36, 1993.
-  Alexander Pinzon and Eduardo Romero.
Análisis experimental de la extracción del esqueleto por contracción con suavizado laplaciano,
December 2010.
Poster presented at 6th International Seminar on Medical Image Processing and Analysis (SIPAIM 2010), December 1–4, Universidad Nacional de Colombia, Bogota, Colombia.

BIBLIOGRAPHY III

-  Alexander Pinzon and Eduardo Romero.
Software para la extracción del esqueleto por contracción y suavizado, December 2011.
Poster presented at 7th International Seminar on Medical Image Processing and Analysis (SIPAIM 2011), December 6–8, Universidad Industrial de Santander, Bucaramanga, Colombia.
-  Alexander Pinzon and Eduardo Romero.
sjskeltonizer: Skeleton extraction software., March 2012.
<http://code.google.com/p/jeronimo/>.
-  Alexander Pinzon and Eduardo Romero.
Shape inflation with an adapted laplacian operator for hybrid quad/triangle meshes.
2013 26th SIBGRAPI Conference on Graphics, Patterns and Images, 0:179–186, 2013.
-  Gabriel Taubin.
A signal processing approach to fair surface design.
In Proceedings of the 22nd annual conference on Computer graphics and interactive techniques, SIGGRAPH '95, pages 351–358, New York, NY, USA, 1995. ACM.
-  B. Vallet and B. Lévy.
Spectral geometry processing with manifold harmonics.
Computer Graphics Forum, 27(2):251–260, 2008.

BIBLIOGRAPHY IV



Yunhui Xiong, Guiqing Li, and Guoqiang Han.

Mean laplace-beltrami operator for quadrilateral meshes.

In Zhigeng Pan, Adrian Cheok, Wolfgang Muller, and Xubo Yang, editors, *Transactions on Edutainment V*, volume 6530 of *Lecture Notes in Computer Science*, pages 189–201. Springer Berlin / Heidelberg, 2011.

THANK YOU FOR COMING TODAY
QUESTIONS?